

# LEAF AREA INDEX ESTIMATION USING LIDAR AND FOREST REFLECTANCE MODELLING OF AIRBORNE HYPERSPECTRAL DATA

Lange, H. and Solberg, S.

Norwegian Forest and Landscape Institute, N-1431 Ås, Norway

## ABSTRACT

Insect-induced damages in forests are a major concern for timber production, landscape conservation and ecosystem research. Early detection methods based on remote sensing data can document the severity and spatial extent of ongoing attacks and might aid in designing mitigation measures or even prevention where necessary. In southeastern Norway, a large-scale insect defoliation of pine trees is ongoing. The larvae of the Pine sawfly *Neodiprion sertifer* create it with its mass attacks during their feeding on needles in June and July. In the winter before the attack, egg galleries are evident in the needles. This provides a test case for early detection methods and remote sensing techniques for monitoring forest health. In the context of an ongoing project on REMote sensing of FORest health (REM-FOR) in Norway, we approach this problem by mapping leaf area index (LAI) before and after the attack in a test area (size around 20 km<sup>2</sup>). LAI is used as a proxy for the crown density, and decreasing trends not related to phenology (non-periodic) indicate defoliation. Estimates for effective LAI for two different years, 2005 and 2007, were derived using airborne laser scanning (LIDAR) calibrated with ground-based point measurements with the LAI-2000 Plant Canopy Analyzer (LI-COR®, USA). These estimates are based on an application of the Beer-Lambert law and a threshold-based separation of laser reflections from the ground and from the canopy [1].

We also obtained airborne high-resolution hyperspectral images (HySpex™, Norsk Elektrooptikk, Norway) for the same reference years to investigate the spectral response of the affected forest. The set of two cameras deliver 330 different spectral channels in the wavelength range 400 to 1800 nm. The analysis might be done using advanced multivariate methods or spectral unmixing using spectral libraries. Here, it was performed using a physically-based model emphasizing geometrical and optical properties of canopies, the Forest Reflectance Model FRT [2]. FRT was designed for the application to (managed) Northern European Forests and is based on conventional forest inventory data, species-dependent parametrized crown shapes, canopy LAI, needle clumping index, and needle optical properties. Here, however, we run the model in an inverse mode, by iteratively minimizing the discrepancy between measured and simulated reflectances,

and predicting the LAI, keeping well-constrained parameters of the model (e.g. tree density, tree height, optical properties of needles) fixed while calibrating others (e.g. needle weight per tree, average shoot length, shoot self-shading). A set of 14 sample trees felled in 2005 further constrain the range of the calibrated parameters, excluding local model inversion minima with unrealistic parameter estimates. The LAI values predicted by the model are then compared to those obtained with airborne laser-scanning with a spatial resolution of 20 m x 20 m for the pine-dominated part of the scenes. In doing so, the spectra from each pixel (size 25 cm x 25 cm) were aggregated by calculating channel-wise median values. In effect, the modelling setup results in determining geometrical and optical properties of forest plots, trees and needles from hyperspectral images. The project data are complemented by images from a range of satellite-based sensors, including MODIS, SPOT, and Hyperion to cover larger regions and as a basis for operationalizing the approach for future insect attacks.

*Index Terms*— hyperspectral images, Lidar, forest health, forest reflectance modelling

## 1. INTRODUCTION

Developing early warning systems for forest health concerns is a desirable goal in forest management. Spatially extended insect attacks can only be tracked using remote sensing methodologies. Depending on scale, availability and precision requirements, either aircraft campaigns or satellite-based products have to be considered. Here, optical imagery, hyperspectral data, laser scanning (Lidar) and synthetic aperture radar (SAR) are most promising at the moment. In the context of a project on forest health and monitoring, an incidence of an insect attack in 2005 (and to a lesser extent in 2007), for which an early warning has been given, was used to initiate a remote sensing campaign. Combining ground-based measurements, laser scanning, and hyperspectral image acquisition, we seek methods for mapping defoliation and possible crown color changes during attack development in the remote sensing data. In this article, two different data sources are investigated: high-density airborne laser scanning and high-resolution hyperspectral images. As a target variable supposed to be

sensitive to changing health conditions, we derived Leaf Area Index (LAI) from laser data obtained prior and after the attack, and from hyperspectral data (after, one-time only) by inversion of a Forest Reflectance Model. These two approaches are completely independent, and we provide a comparison of the resulting LAI estimates.

## 2. MATERIALS AND METHODS

### 2.1. Study site

The study area is a pine-dominated relatively open commercially used forest of varying tree density, located in Åsnes municipality, Hedmark county, southeast Norway (ca. 60°41' N, 12°18' E). In autumn and winter 2004, an infestation of pine trees with the European pine sawfly (*Neodiprion sertifer*) has been observed, with an outbreak in the summer of 2005 and some again in 2006 and 2007, although weaker and partly at another site. Visual inspection in late 2005 revealed a partial or near-total crown defoliation, most pronounced for last year's needles.

### 2.2. Remote sensing data

Airborne laser scanning with a density of around 2 pulses per m<sup>2</sup> was performed just prior to the attack (in May), just after it in late July, and after a recovery period in September, covering an area of around 20 km<sup>2</sup>, with an Optech ALTM 3100 Lidar scanning system. A flight with a hyperspectral camera (HySpex™, Norsk Elektrooptikk, Norway) was performed in late August 2005. Two different resolutions were obtained, with an effective pixel size of 25 cm x 25 cm in the wavelength range 400 to 1000 nm, and 1 m x 1m for the range 1000 to 1800 nm. For the sake of simplicity, we report on the higher resolution data only; the data being distributed over 160 channels with a spectral resolution (full width half maximum) of around 2.5 nm.

The data collection of the project contains also multitemporal satellite data (MODIS, SPOT, and Hyperion), LAI measurements with Licor plant canopy analyzer LAI-2000, and tree physiological data obtained from 14 felled sample trees, utilized in another part of the project. They do, however, constrain the parameter range of the FRT model (cf. sec. 2.6).

### 2.3. Laser-based LAI estimation

Based on the Beer-Lambert extinction law, gap fractions were calculated by subdividing the pulse returns into ground and canopy hits, with a threshold of 1 m. The logarithm of the ratio of the number of total returns to ground returns is proportional to LAI [1]. The scale (size of reference area) for the LAI values may vary, but accuracy and stability of the results depends on that choice. Here, a map of LAI values with a 10 m x 10 m raster was used. With the chosen

threshold of 1 m, individual grid cells may receive an LAI value of exactly zero.

### 2.4. Single tree masking

As we are mostly interested in reproducing reflectance spectra from (pine) trees only, the Lidar data were also used to discern trees from other vegetation and non-vegetated ground. For that purpose, a single tree segmentation algorithm [3] was performed: a canopy surface model with a 25 cm x 25 cm grid was created, and a local maxima (highest height value within the immediate grid neighbourhood) search performed. A modified watershed algorithm produced polygons delineating individual tree crowns, but possibly also other non-tree segments. As trees we selected only segments having a maximum higher than 2 m. Visual inspection revealed further that there was a positional mismatch between polygon centers and obvious tree tops in the hyperspectral orthoimages and the Lidar-based segments, because the orthophoto was georeferenced at the ground and not at the canopy surface. To cope with this, a 50 cm buffer zone was provided on the inside and outside of each polygon, reducing the risk to extract pixels attributed to trees actually belonging to ground. On the other hand, the number of trees remaining is also reduced - an effect which is largest for trees with small crowns.

### 2.5. Preparing the hyperspectral data

A test scene (Fig. 1) of dimensions 600 m x 800 m was selected, and corresponding pixels with hyperspectra extracted. These data were then masked using the buffered tree polygons (an example is shown in Fig. 2), i.e. only the interior of each polygon with a tree height > 2 m retained. Tree density is substantially varying within the scene. To avoid areas with no or just a single tree, we aggregated to 20 m x 20 m plots, aligned with the Lidar-LAI raster; the latter were arithmetically averaged using the four corresponding 10 m x 10 m plots.

The number of plots was further reduced using a forest stand map, retaining only plots with more than 80% of the trees being pine. This does not, however, guarantee that only pine trees are contained in the selection. In total, we retrieved 382 plots.

It is known that the 160 spectral channels contain a lot of redundant information. On the other hand, the performance of the forest reflectance model is inversely related to the number of channels. We therefore made a selection of channels which are supposedly least redundant, following in part the PCA-based results obtained in [4] and own investigations on spatial variability. In total, we used 35 channels in the range 400 nm to 1000 nm, most finely sampled around the red edge and most coarsely in the near infrared part.

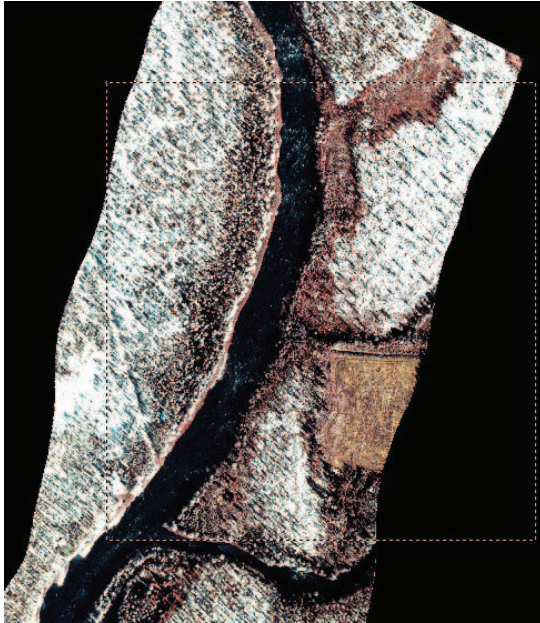


**Figure 1:** The selected hyperspectral scene containing a mixture of age classes, stand density, and non-forested areas, and the rectangle where individual tree polygons were calculated. The size of the rectangle is 600 m x 800 m, the coordinates of its upper left corner are (6735015 N, 353590 E) in UTM zone 33 N.

For each 20 m x 20 m plot, the hyperspectra of all pixels inside tree polygons were aggregated to a single average spectrum as required by the FRT model. In order to minimize the impact of possible ground vegetation “contamination”, we used the channel-wise median value.

As a final step, the radiation data were converted to reflectance values, using two white reference membranes laid out in the field during the flight, using the arithmetic average of all pixels covering the membranes. This simple recipe may be a limitation, since light conditions (in particular, the dark current) may vary locally and temporally, although cloud cover was minimal. Much more elaborate reference reflectance measurements are reported in [4].

## 2.6. The FRT model

The interpretation of reflection data from the ground and vegetation requires a modelling framework which comprises radiation theory, atmospheric corrections, geometric properties of needles, shoots, stems and other vegetation parts, and utilizes available information on tree species, stand age, ground vegetation type, and others. We used the Forest Reflectance and Transmittance (FRT) model [2,5], in which 45 parameters are tunable for the calibration of atmospheric corrections, leaf optics, self-shading and clumping, biomass distribution and stand geometry.

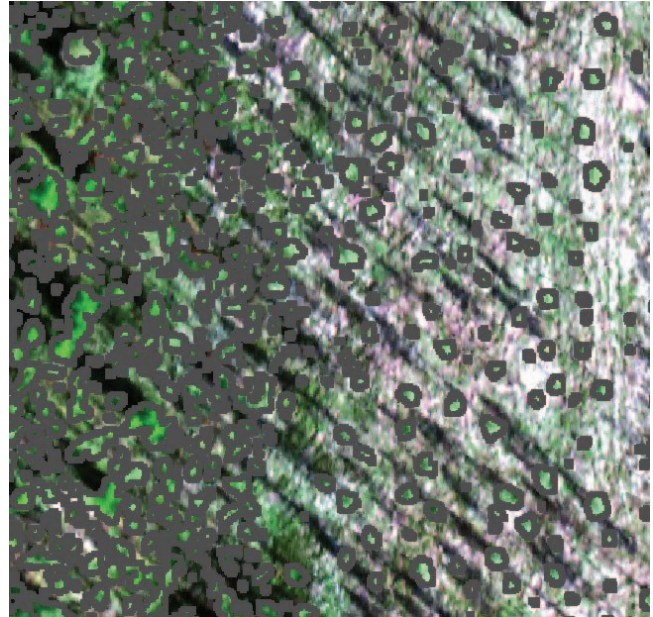


**Figure 2:** Example of single tree delineation used to mask the hyperspectral data. The thickness of the polygon borders is according to the buffering described in the text. In the right half of the image, polygons are visible which occur at the tip of the stretched shadows, indicating a correct localization of the individual crowns. All data outside the polygons are ignored in the FRT modelling.

To the extent possible, tree species-related properties such as needles, branches and trunks optical behavior, specific needle weight, and atmospheric correction parameters were kept fixed at calibrated values (for example, trunk reflectance data for pine trees were available). Ground vegetation and soil contributions to total reflectance were kept at a minimum, e.g. by attributing a LAI value of 0.01 to the upper ground vegetation layer, since these compartments were deliberately excluded through the selection procedure (sec. 2.5). This is a crucial point since it is known that their properties have a big impact on reflectance estimates otherwise, and their treatment requires special care and is tedious [6].

We run the model in the inverse mode where LAI and other properties are determined by trying to match the observed reflectances from the 35 channels in an iterative procedure for each plot separately in an automated fashion. The modeller has to choose the adjustable parameters in order to obtain the match; this is not an easy task since convergence properties, performance and quality of the simulation (expressed through a merit function) crucially depend on that choice. In this work, we allowed five parameters to vary freely: stand density, average tree height (per plot), crown radius, the ratio of Branch Area Index to LAI and the tree grouping index.

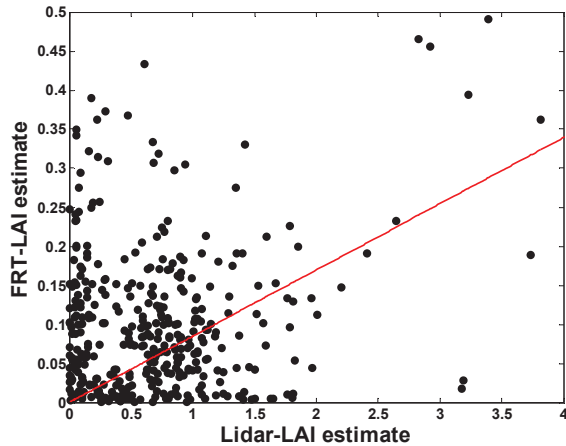


**Figure 3:** Comparison of LAI estimates: the laser-based LAI values from the flight in July (after the attack) versus the FRT model estimates from the hyperspectra, rescaled to 20 m x 20 m plots;  $R^2=0.22$ . For the Lidar data prior to the attack (obtained in May), we obtain  $R^2=0.15$ . The solid line is a linear regression with a forced zero intercept.

### 3. RESULTS

FRT model simulations led to very reasonable estimates for mean tree height and crown radius (although a detailed validation was not possible at this stage). The tree grouping estimates point to regular (as opposed to clumped or random) stands, which is fully plausible. The simulated reflectance spectra (not shown) differed a lot in quality, but had the common feature to generally underestimate the observations. The estimated LAI values refer to the tree segments only. A majority of the pine trees were tall, and the model had a tendency to obtain a value around 0.8 for them, which is plausible given the Licor LAI-2000 reference measurements. However, in order to compare with the Lidar LAI estimates which refer to the whole of each plot, the FRT estimates were rescaled to each 20 m x 20 m plot by multiplying with the corresponding tree cover fraction. The latter was largely different between plots (ranging from less than 1 percent up to 64 percent of the pixels). This implies the assumption that other parts of the plot do not contribute to the total LAI, leading to a clear underestimation of LAI. This problem is rather obvious from Fig. 3 (consider the scale of the two axes). However, there is at least a clear correlation between the two data sets, which was not obvious from the start since the approaches to obtain LAI were completely different. The scatter is most pronounced for small LAI values, typically corresponding to a very small number of trees in the plot and thus little reliability; the relation seems to tighten for larger values. When using laser data prior to the attack (not shown), the correlation is weaker as expected, since the hyperspectral data were obtained later (in August).

### 4. DISCUSSION

We exploited the FRT model in an automatic fashion for a larger region. Parameter estimates obtained are plausible. The problem of underestimating LAI in particular for sparse regions can be overcome by either working in dense forests, or taking ground vegetation into account (which requires a lot of additional ground truth data). However, to use these reconstructions in a forest health monitoring context, the main objective of the REMFOR project, requires repeated hyperspectral measurements, which were not available here.

### 5. ACKNOWLEDGMENTS

We express our thanks to Dr. Andres Kuusk (Tartu Observatory, Estonia) for providing us with the source codes for the FRT model, Dr. Tiit Nilson from the same institute for discussions on the modelling procedure, the companies NEO (Norsk Elektrooptikk) and Blom Geomatics for performing the flights and initial data processing. The Norwegian research council, the Norwegian Ministry of agriculture and food, and the “Skogtiltaksfondet” funded by the Norwegian forest owners are all acknowledged for their financial support of the REMFOR project.

### 6. REFERENCES

- [1] S. Solberg, E. Næsset, K.H. Hanssen and E. Christiansen, “Mapping defoliation during a severe insect attack on Scots pine using airborne laser scanning”, *Remote Sensing of Environment*, Elsevier Inc., vol. 102 (3-4), pp. 364-376, 2006.
- [2] A. Kuusk and T. Nilson, “A Directional Multispectral Forest Reflectance Model”, *Remote Sensing of Environment*, Elsevier Inc., vol. 72 (2), pp. 244-252, 2000.
- [3] S. Solberg, E. Næsset and O.M. Bollandsås, “Single-tree segmentation using airborne laser scanner data in a structurally heterogeneous spruce forest”, *Photogrammetric Engineering and Remote Sensing*, American Society for Photogrammetry and Remote Sensing, vol. 72, pp. 1369-1378, 2006.
- [4] P.S. Thenkabail, E.A. Enclona, M.S. Ashton and B. Van Der Meer, “Accuracy assessments of hyperspectral waveband performance for vegetation analysis applications”, *Remote Sensing of Environment*, Elsevier Inc., vol. 91 (3-4), pp. 354-376, 2004.
- [5] T. Nilson, A. Kuusk, M. Lang and T. Lökk, “Forest Reflectance Modeling: Theoretical Aspects and Applications”, *Ambio*, Allen Press Inc., vol. 32 (8), pp. 535-541, 2003.
- [6] P. Weihs, F. Suppan, K. Richter, R. Petritsch, H. Hasenauer and W. Schneider, “Validation of forward and inverse modes of a homogeneous canopy reflectance model”, *International Journal of Remote Sensing*, Taylor & Francis group, vol. 29 (5), pp. 1317-1318, 2008.